Comprehensive analysis of multiple asphaltene fractions combining statistical analyses and novel visualization tools

Mary J. Thomas[1,2], Hugh E. Jones[1,2], Diana Catalina Palacio Lozano[2], Rémy Gavard[1,2], Shaun Carney[3], Mark P. Barrow[2*]

1. Molecular Analytical Sciences Centre for Doctoral Training, University of Warwick, Coventry, CV4 7AL
2. Department of Chemistry, University of Warwick, Coventry, CV4 7AL
3. Lubrizol Ltd., Hazelwood, Derby, DE56 4AN

*Corresponding Author m.p.barrow@warwick.ac.uk

Abstract

Marine heavy fuel oils (HFOs), derived from and often blended with hydrotreated residual cuts, typically possess high boiling point, viscosity, and molecular complexity, and so are inherently challenging to analyze at the molecular level. Their high asphaltene content is associated with undesirable phenomena including flocculation, deposition, and black paint formation in marine engines. Asphaltene fractions of eight HFOs were selected for analysis by Fourier transform ion cyclotron resonance mass spectrometry (FTICR MS) due to their differing behaviour, including responsiveness to additive chemistries designed to stabilise against asphaltene handling issues. A selected mass region was isolated and fragmented using infra-red multiphoton dissociation (IRMPD), and the relative heteroatom content in asphaltene cores and smaller aromatic moieties, and degree of alkylation and aromaticity, of

the fragments generated for each sample compared. A more extensive elucidation of the molecular-level differences between the n-alkane insoluble asphaltene fractions is afforded, with key components underlying variation in bulk behaviour identified through statistical approaches. The approach presented allows additive packages to be adjusted to address asphaltene handling issues presented by more challenging samples, and simpler and more ubiquitous formulations may eventually be developed.

Abbrevivations: Atmospheric pressure chemical ionization, APCI; Atmospheric pressure photoionization, APPI; Collision induced dissociation, CID; Double bond equivalents, DBE; Electrospray ionization, ESI; Fourier transform ion cyclotron resonance mass spectrometry, FTICR MS; Heavy Fuel Oil, HFO; Hierarchical clustering analysis, HCA; International Maritime Organization, IMO; Infra-red multiphoton dissociation, IRMPD; Molecular weight, Mw; Polycyclic aromatic hydrocarbon, PAH; Principal component analysis, PCA; Saturates, aromatics, resins, and asphaltenes, SARA; Tandem mass spectrometry (MS/MS)

Keywords: Marine HFOs; asphaltenes; desulfurization; Fourier transform ion cyclotron resonance; mass spectrometry; additive packages

1. Introduction

Petroleum-related samples are ultra-complex mixtures for which detailed compositional analysis at the molecular level is only feasible through the use of ultra-high resolution mass spectrometry techniques [1-3]. Petroleum may be divided into four fractions based on their polarity and solubility: saturates, aromatics, resins and asphaltenes (SARA) [4]. Asphaltenes are typically defined as the fraction of petroleum insoluble in n-alkanes such as n-heptane, but soluble in toluene [5]; the classical physical model of petroleum considers asphaltenes as solute, with the remaining SAR fractions acting as non-solvent, solvent, and dispersant respectively [6]. Asphaltenes are prone to flocculation when above a critical concentration, or when they are components in an incompatible blend [7, 8]. The resultant deposition can lead to pipeline blockages, impeding pigging or necessitating it at more regular intervals, and undesirable black paint formation in marine engines [9, 10]. Additive formulations can help stabilise marine heavy fuel oil (HFO) against black paint formation [11], although performance varies owing to global variations in HFO composition.

Further compounding handling problems such as black paint formation, asphaltenes can also act as inhibitors in desulfurization processes [12]. Desulfurization efficiency is of growing importance with restrictions on sulfur content in HFOs tightening in line with regulations set by the International Maritime Organization (IMO) 2020 [10, 13]. Inhibition of treatment processes, including desulfurization, may be attributed to basic nitrogen-containing species and aromatic compounds [14, 15]. As the large stable aromatic cores of asphaltenes are capable of stabilizing charge through delocalization [16], and terminating free radical reactions through recombination and disproportionation [17], they may also present an

impediment in some desulfurization processes, particularly where transformation of co-occurring refractory aromatic sulfur compounds is required [15].

Solvent extraction in n-heptane is commonly used for asphaltene fractionation [10], and Soxhlet extraction is routinely used to obtain hydrophobic components, including petroleum-related substances, from soil [18, 19]; such techniques may be utilised in order to study the n-alkane insoluble compounds, including asphaltenes, isolated from whole oils. While the molecular-level structure of asphaltenes is still not fully understood [10], they are now widely considered to comprise polycyclic aromatic hydrocarbon (PAH) cores [20] with average molecular mass around 750 Da. Asphaltenes often containin heteroatoms such as N, O, or S [21, 22], which may exacerbate handling issues, cause catalyst fouling, or alter responsiveness to additives [10, 23]. Island and archipelago-type asphaltenes, defined as a single PAH cores substituted with alkyl chains or multiple PAHs bridged by alkyl linkers, respectively, have both been detected [24-26]. Interpretation of asphaltene core structure, and comment on the likely predominance of island or archipelago-type asphaltenes using Fourier transform ion cyclotron resonance mass spectrometry (FTICR MS) analyses has previously included inspection of fragment ion spectra, comparison of average molecular weight (Mw), plots of double bond equivalent (DBE) against carbon number, and DBE distributions [25-29]. Atmospheric pressure photoionization (APPI) provides the most extensive compositional coverage for the study of heavier oils [30-32] and their asphaltene fractions [33, 34], as it more efficiently ionizes non-polar and aromatic compounds [33, 35] due to a lower reliance on ion-molecule chemistry, and is less susceptible to ion suppression than other techniques including electrospray ionization (ESI) and atmospheric pressure chemical ionization (APCI) [36, 37].

Tandem mass spectrometry (MS/MS) methods can be used to elucidate structural information by, for example, utilising quadrupole isolation to select precursor ions, before producing fragments using a neutral collision gas [38]. Although collision-induced dissociation (CID) is used widely, proceeding via vibrational energy pathways which makes the method selective towards cleavage of the weakest bonds [39], there are several limitations to this technique. For instance, more efficient fragment generation is offered through the use of heavier neutral collision gases, however the costs associated with these often limits the user to lighter gases such as nitrogen or argon, where multiple collisions may be required to generate fragment species of interest [40]. Furthermore, the increase in ion kinetic energy required to induce dissociation in CID can limit the observation of low *m/z* product ions [41, 42]. Following precursor selection, fragment ions generated by CID in the collision cell must then be transferred to the ICR cell, such that, without careful tuning, m/z range biases and ion losses can occur, resulting in failure to detect lower abundance species. In infra-red multiple-photon dissociation (IRMPD) the ion energy is increased by photon absorption, while fragmentation occurs inside the ICR cell [43], overcoming ion transfer issues. Although IRMPD involves the absorption of infrared photons and CID involves collisions, both methods proceed via increasing vibrational energy of the ion. IRMPD in the ICR cell has the advantages of not increasing the pressure, which adversely affects instrument performance, and can yield secondary fragmentation. The detection of lower molecular weight species and sensitivity to lower abundance species is improved. IRMPD has been used to access core structures of asphaltenes of mass-selected isolation windows [26].

Consistent boundaries have been used to define regions of nitrogen-class DBE plots by the possible structure of aromatic cores [23]. Although a precise definition of the compositional boundaries for island and archipelago-type asphaltenes has not yet been attained, it is possible to keep experimental procedures constant between analyses and use consistent compositional boundaries for comparisons of samples. Such an approach allows for differences in ionization efficiency between the two structures [24]. Following fragmentation both neutral and ionic fragments will be generated, with highly condensed asphaltene cores or smaller aromatic moieties detected depending on which carries the charge from the precursor. An assessment of predominance of island or archipelago structures is made, as well as determination of predominant heteroatom situation in asphaltene cores or in smaller aromatic moieties. Fragments indicative of island-type asphaltene precursors are considered to be those with similar DBE to parent ions [28].

HFOs properties are typically assessed using bulk analytical techniques, however molecular-level profiles cannot be elucidated using these methods. In this work, Soxhlet extraction was performed using n-heptane to optimize the isolation of the asphaltene fraction of eight HFO samples. The asphaltene fractions were then analysed using (+) APPI–FTICR MS and IRMPD fragmentation. Principal component and hierarchical clustering analyses (PCA and HCA), used widely for fingerprinting petroleum-related samples [15, 16, 44-50], were performed on asphaltene fragment data. The location of variables relative to the circle of correlations in a PCA loadings plot are used to determine heteroatom class groups which contribute most significantly to the differences between samples [51], allowing the molecular-level features that are common in HFOs exhibiting problematic behaviour to be determined.

Combining statistical approaches with DBE and carbon number distributions presented in a novel, simultaneous, manner for multiple fragment compound classes, affords a comprehensive characterisation and comparison of HFO asphaltene fractions. This improves understanding of HFO bulk behaviour in the field, as well as their responsiveness to additive chemistries designed to stabilise them against asphaltene handling problems.

2. Material and methods

2.1 Soxhlet Extraction (C_7 Soxhlet asphaltenes)

Eight HFOs (A to H) (Lubrizol Ltd, Derby, UK), selected for differences in bulk behaviour across a range of bulk asphaltene content (Table S1), were provided for compositional analysis. Soxhlet apparatus containing each HFO and ~100 mL of n-heptane (Fisher Scientific, Hemel Hempstead, Hertfordshire, United Kingdom) were heated to 130 °C for 22 h. The solid asphaltene residue remaining on the filter was dissolved in toluene (Honeywell Speciality Chemicals Seelze GmbH, Hanover, Germany) and filtered prior to direct infusion experiments.

2.2 FTICR MS

C_7 Soxhlet asphaltene fractions isolated from HFO samples A-H were dissolved in toluene (Honeywell Speciality Chemicals Seelze GmbH, Hanover, Germany). Mass spectra were acquired using a 12 T solariX Fourier transform ion cyclotron resonance (FTICR) mass spectrometer (Bruker Daltonik GmbH, Bremen, Germany), coupled to an APPI II source operated in positive-ion mode. Nitrogen was used as the drying gas at a temperature of 220 °C and at a flow rate of 4 L min^{-1}. The nebulizing gas was nitrogen and was maintained at a pressure of 1.2 bar. A krypton lamp was used to produce photons with energy 10.6 eV.

Samples were introduced by direct infusion using a syringe pump at a rate of 1000 μL h^{-1} without the activation of in-source dissociation. Low concentration tuning mix (Agilent Technologies, San Francisco, CA, USA) was used as an external calibrant. 4 M data sets were acquired in the detection range *m/z* 147-1800 for 300 scans. The data were zero-filled once and apodized using a Sine-Bell function prior to applying a fast Fourier transform. For apodized data, the measured resolving power at *m/z* 400 was typically 450,000 to 850,000 depending on the sample studied. IRMPD experiments were performed on an isolation window of an *m/z* width of 50 centered on *m/z* 564 using a continuous wave, 25 W, CO_2 laser (Synrad Inc., Washington, USA) operating at 60% power output. Photons were produced at a wavelength of 10.6 μm and pulsed into the ICR cell for 0.8 s prior to detection with the low mass cut-off (LMCO) lowered to *m/z* 98.3. The spectra were phased with a Half Hanning apodization setting of 0.18 – 0.6 before baseline correction using FTMS Processing 2.1.0 (Bruker Daltonik GmbH, Bremen, Germany). Phased spectra were internally calibrated using homologous series and analyzed using DataAnalysis 4.2 (Bruker Daltonik GmbH, Bremen, Germany), prior to the data being imported into Composer 1.5.6 (Sierra Analytics, Modesto, CA, USA) for compositional analysis, searching for homologous series within elemental constraints (Table S2) with a maximum assignment error of 1 ppm permitted. Mass lists generated from IRMPD spectra were cut to remove peaks above m/z 537.5. To more effectively perform PCA and HCA analyses and to simplify visualization, compound classes were grouped according to heteroatom content. $N_nO_xS_y$ labels were used to denote groups of heteroatom classes where one class possessed n, x or y in excess of 1. Aabel NG2 v.5.2 (Gigawiz Ltd. Co., Tulsa, Oklahoma, USA), OriginPro 2016, and KairosMS (University of Warwick, Coventry, UK) in-house software was used for data categorization, visualization, and statistical analysis. RStudio program (RStudio Inc., Boston, Massachusetts, USA) was used for

PCA analysis using dudi.pca from the ade4 package and visualized using fviz_pca from the factoextra package, and HCA analysis was carried out using agglomerative clustering and the Canberra method.

3. Results and Discussion

3.1 C_7 Soxhlet Asphaltene Fractions of HFOs A-H

The asphaltene fractions from eight HFO samples isolated by Soxhlet extraction in n-heptane were compared for an overview of compositional differences. The grouped class distribution for the asphaltene fractions of HFOs A-H is shown in Figure 1, with the individual class distribution data shown in Figure S1.

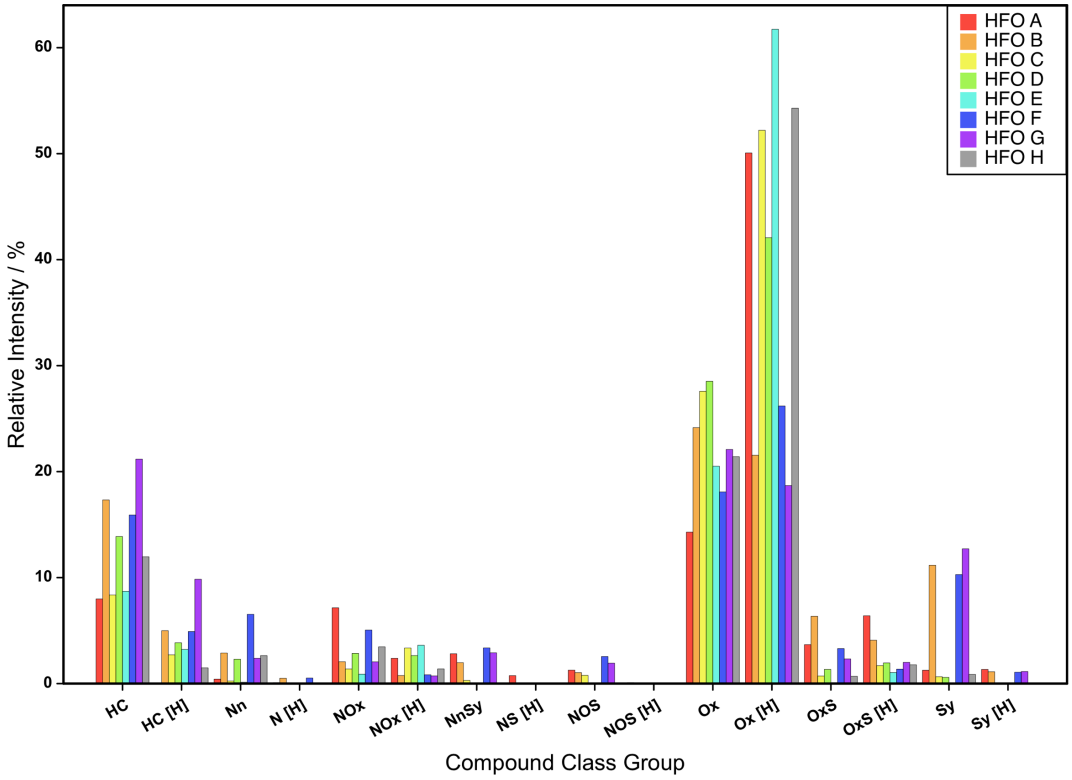

Figure 1 – Grouped compound class distribution for C_7 Soxhlet asphaltene fractions of HFOs A-H.

For HFOs A, C, E, and H, a relatively strong contribution was observed for oxygen-containing classes, particularly O_x[H] classes. HFO E appeared to have a correspondingly lower contribution from the HC, HC[H] and N_n classes, while the majority of S-containing classes were not detected for the asphaltene fraction of this sample. HFO E has a lower sulfur content; it is possible that it was inherently lower in sulfur, was blended with a distillate cut to lower its sulfur content, or, given the strong contribution from oxygen-containing classes, had undergone a desulfurization process involving an oxidation step. A crude oil control sample was run on on the same day as the HFO samples and evidences a far lower contribution from oxygen-containing classes (Figure S2). Furthermore, there is significant variation in the contributions from the oxygen-containing classes between samples in Figure

1. The combined evidence allows us to conclude with confidence that these oxygen-containing classes are sample-related and do not arise as a result of oxygen adduct formation during (+) APPI ionization.

The class distributions of the asphaltene fractions of HFOs B, F, and G appear similar, in particular the strong contributions from S-containing classes. However, several observations that may explain differences in bulk behaviour can be made. For example, HFO F appears to have a greater relative contribution from several nitrogen-containing classes, particularly N_n, N[H], and NO, which may be important for responsiveness to additive chemistries designed to stabilise HFOs against asphaltene flocculation, deposition and black paint formation. HFO G appears to have a strong contribution from the HC and HC[H] classes, while HFOs B and G have a strong contribution from the O class. O-containing compounds, which may include some asphaltenes, can affect responsiveness to additive chemistries due to their interactions with the polar, O-containing functionalities on additives such as dispersants [52]. The HC[H] class makes a less substantial contribution to the other asphaltene fractions, indicating that the hydrocarbon substances present in HFO G may differ to those present in other samples and cause handling issues.

HFO H has a relatively strong contribution from the NO class, similar to HFOs A and F, and from the O_x[H] classes, similar to HFO E, and in contrast to the high contribution from the O class observed in problematic HFOs B and G. Low sulfur contents coupled with relatively high oxygen content have been observed in lacustrine-derived oils [53]. These similarities between HFOs that are known to respond well to additive chemistry, or those with a low sulfur content, may be responsible for the absence of apparent asphaltene handling issues for HFO H.

Demonstrating the efficiency of the C_7 Soxhlet fractionation, the distribution of DBE detected in the S class of the asphaltene fraction of HFO A is compared to that detected in the whole oil and its maltene fraction in Figure 2. The data is broken down further into plots of DBE against carbon number in Figure S3.

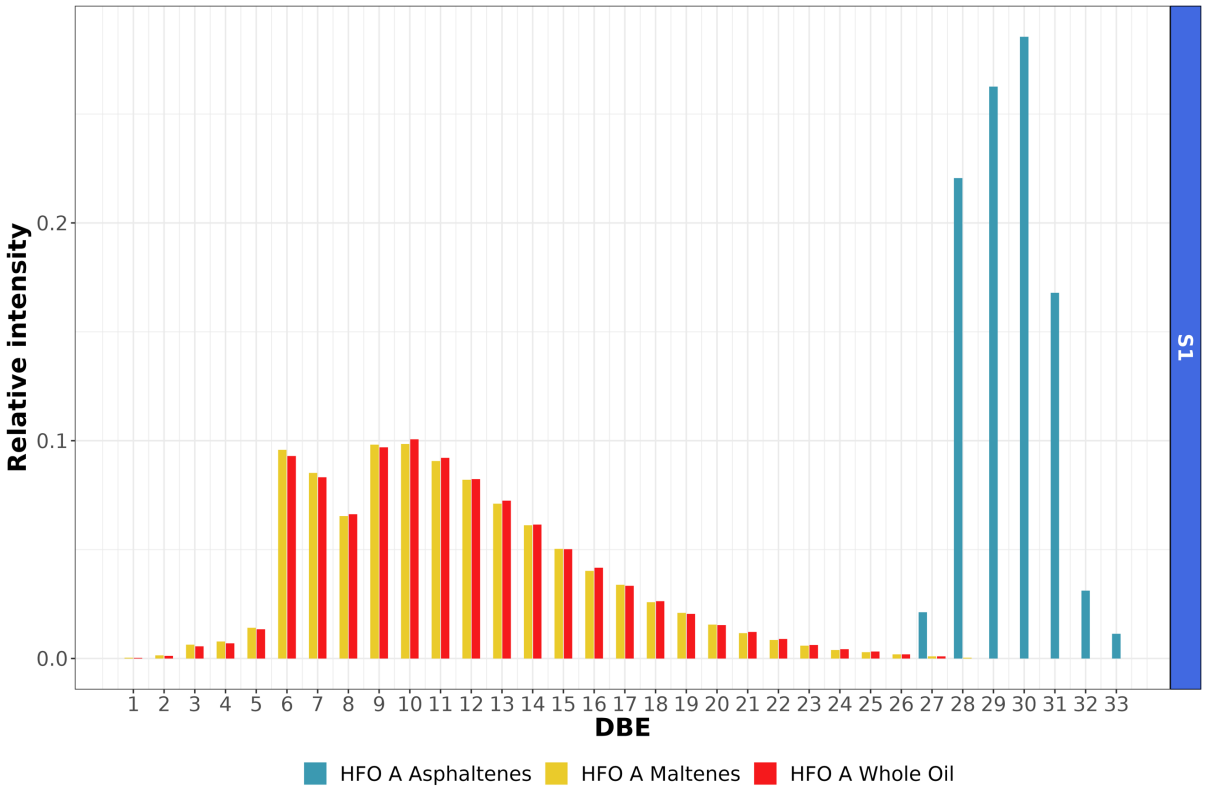

Figure 2– Distribution of DBE values of the S class, compared between whole HFO A, and its maltene and asphaltene fractions, demonstrating the efficient isolation of the asphaltene fraction using Soxhlet extraction

The S class DBE distribution shown in Figure 2 demonstrates the expected similarity between species detected in the whole HFO and the maltene fraction, which may result from a predominant detection of aromatic fraction species when studying whole oils [54]. There is a

large increase in contribution to relative intensity beginning from DBE 6, corresponding to the minimum required to form a benzothiophenic species. Figure 2 also shows that higher DBE species were detected in the asphaltene fraction such that the compositional space of the HFO accessible was extended following separation. Efficient isolation of highly aromatic, high DBE asphaltene species has also been demonstrated following development of separation procedures, with different DBE ranges accessed depending on fractionation conditions [27]. A less selective separation method of dissolution of whole HFOs in dodecane followed by filtration of the insoluble fraction (C_{12} asphaltenes) provided access to higher DBE species of up to 32, but did not efficiently separate these from the bulk of the sample, such that the strongest relative contribution to the S class was from DBE 6 (Figure S4). The similarity between whole HFO A and its C_7 Soxhlet maltene fraction is demonstrated further in the class distribution data presented in Figure S5.

3.2 IRMPD Fragmentation of HFO A-H Asphaltene Fractions

To gain an understanding of whether heteroatoms are primarily contained within stable, highly condensed asphaltene cores, or in smaller aromatic moieties, MS/MS spectrometry experiments were performed. Precursor ions isolated in a window of width *m/z* 50 centered on *m/z* 564 were subjected to IRMPD fragmentation. Example fragment spectra are shown in Figure S6. Narrower isolation windows, for example of width *m/z* 2 [23], can be used to fragment selected species for detailed structural information, however in this case a broader comparison of asphaltene fraction compounds in several samples was obtained. Lower abundance species are detected more readily and greater resolving power is afforded in isolation mass spectra compared to broadband mass spectra [1]. This can be demonstrated

by the relative abundance of N_nS_y classes, which are only detected in the broadband mass spectra of HFO A, but detected in the isolation spectra of several HFOs (Figures S1 and S7).

The change in relative intensity of compound class groups comparing fragmentation spectra to the corresponding precursor isolation spectra for each HFO is shown in Figure 3. The individual and grouped class distribution data used to generate Figure 3 are shown in Figures S7-9. A change in heteroatom class assignment occurs when the fragments detected contain fewer heteroatoms than the precursor parent ions. A negative change in relative intensity indicates that a compound class group is detected at lower relative intensity in the fragmentation spectra compared to the precursor ion isolation spectra, indicating that such species fragment more readily.

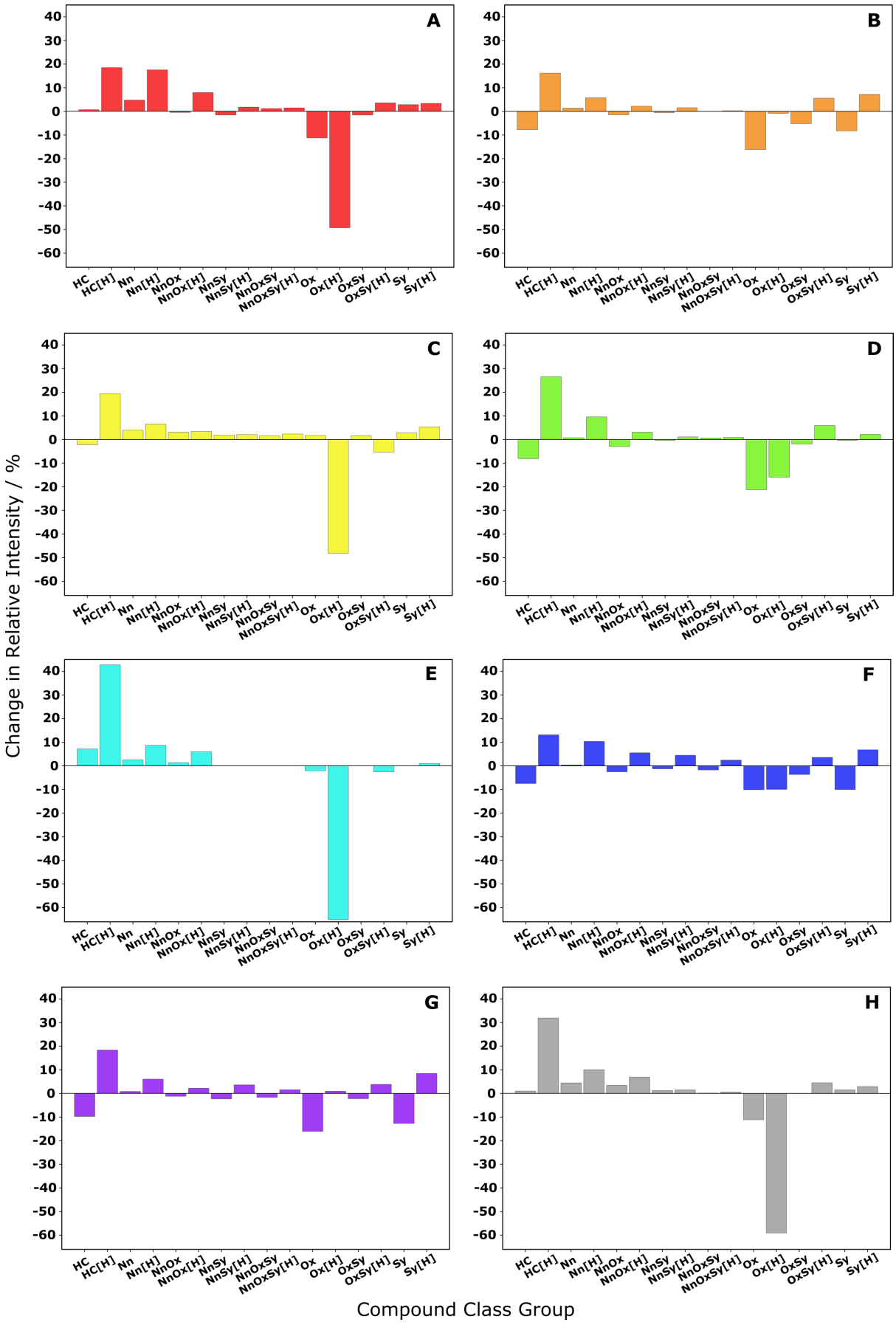
A
B
C
D
E
F
G
H
Change in Relative Intensity / %
Compound Class Group
HC
HC[H]
Nn
Nn[H]
NnOx
NnOx[H]
NnSy
NnSy[H]
NnOxSy
NnOxSy[H]
Ox
Ox[H]
OxSy
OxSy[H]
Sy
Sy[H]

Figure 3 – Change in relative intensity of compound class groups following IRMPD fragmentation

Figure 3 shows that generally, a shift from radical (odd-electron) to even-electron classes is observed following fragmentation, which is due to the greater reactivity of radical precursor species causing them to fragment more readily. Following IRMPD fragmentation, the largest decrease in the relative intensities was observed for the O_x[H] classes for several HFOs, most notably for HFOs A, C, E, and H. This is likely due to these classes comprising functionalities including carboxylic acids, which are capable of forming good leaving groups such as OH, COOH, CO_2 and H_2O. As a result, a shift from O_x[H] predominance to O_x or HC and HC[H] classes is observed. HFOs B and G, on the other hand, appear to have had a similar change in the relative intensities of compound class groups, with a more pronounced decrease in the O_x and S_y classes.

Figure 1 showed that the broadband asphaltene spectra of HFO E had low relative contribution from the N_n and N[H] classes, however Figure 3 indicates that N_n[H] class fragment ions have been generated for HFO E. These may be derived from parent ions containing more than one heteroatom, for instance those assigned to NO_x[H] classes. For HFO F, N-containing classes were detected in both the broadband asphaltene mass spectrum and the IRMPD fragment spectrum. While N-containing precursor ions were detected in relatively high abundance for HFO F, a considerable contribution from N_n and N_n[H] fragment ions was also detected, as demonstrated by the positive change in intensities indicated in Figure 3. The contribution from HC and HC[H] fragments is comparatively low, suggesting that nitrogen-containing functionality is retained in the fragments generated.

HFOs E and H have a sharp increase in HC[H] relative intensity following fragmentation, which suggests that the precursors isolated for these samples, predominantly O_x[H] species, may be more likely to have heteroatoms present in substituent chains or leaving groups rather than in stable aromatic cores. Although HFO A also had a strong contribution to its precursor ion spectrum from O_x[H] classes, it also had a relatively high contribution from the NO class, similar to HFOs D and F, and these appear to have generated a greater relative proportion of N_n[H] class fragment ions.

Class distributions alone do not indicate whether heteroatoms are contained within highly condensed aromatic cores or in smaller aromatic moieties, as the fragment that carries charge, and is therefore detected, may not necessarily be the asphaltene core. The relative ability of fragments generated to stabilise charge influences the ion classes observed and their relative abundances. The increase in molecular energy imparted by absorption of a photon during IRMPD induces cleavage of the weakest bonds through increased vibrational energy, such that at low laser energies the mechanism is comparable to that observed in CID. Alkyl chain cleavage, resulting in loss of substituent chains from the aromatic core, is therefore the predominant fragmentation mechanism [27], and depending on which carries charge either may be detected as ionic species in the fragment spectrum.

Figure 4, which visualizes the spread of DBE for selected heteroatom classes simultaneously using boxplots, demonstrates a novel means by which to compare the predominant heteroatom location in the fragments detected. The boxplots are compared against the intensity weighted mean, and maximum and minimum DBE, of all precursor ions detected

prior to fragmentation. Additional DBE and carbon number information, for a wider range of fragment ion classes, is presented in Figure S10. Fragments with higher DBE are likely to be stable, highly condensed, aromatic cores that have undergone alkyl losses. By contrast, those with lower DBE represent smaller aromatic moieties. Comparison of asphaltene fragments for structural information is typically performed through comparison of multiple plots of DBE against carbon number [26], which is time consuming and makes cross referencing challenging.

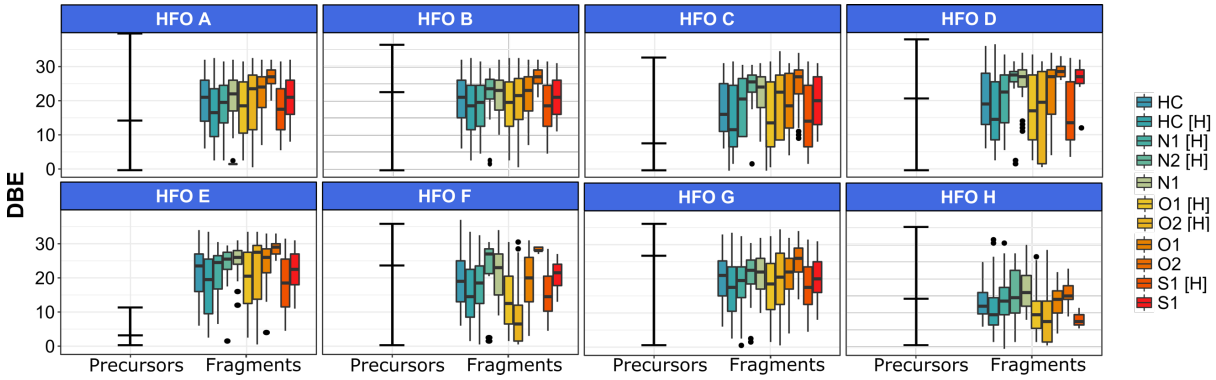

Figure 4 – Intensity weighted mean and boxplots showing range of DBE in selected fragment ion classes. The intensity weighted mean and range of DBE for all precursor ions detected in the isolation spectra is indicated for comparison.

Figure 4 and Figure S10 provide a rapid and simplified comparison of multiple fragment DBE and carbon number distributions, and are less time consuming to inspect than DBE plots generated for individual heteroatom classes and samples. While the average carbon number for precursors is similar across all samples, HFOs A, C, and E precursors have low mean DBE. This could be due to the lower asphaltene content and higher proportion of oxygenated compounds detected in these samples, such that the heptane-insoluble fraction, and consequently precursor isolation spectra, instead comprises highly polar and alkylated

species. Given the inherent complexity of HFOs and the range of processes they undergo, the asphaltene fraction isolated through insolubility in n-alkanes could be mixed with complex feedstock sources. For HFO E polar species may be particularly predominant if the HFO has undergone a desulfurization process involving oxidation, while generation of fragments with higher DBE than precursors may be due to rearrangement reactions of these species following photon absorption. Nevertheless, some fragments that may be related to asphaltene core structure can be visualized and compared between all samples. Over 70% of the relative intensity of the precursor ion NO class is assigned to species with DBE of 25 or above (Figure S11), so as a rough approximation, fragment ions maintaining DBE over 25 are considered to be derived from island-type asphaltene precursors.

High DBE fragments containing nitrogen, that are likely to represent content in asphaltene core structures, were detected in the majority of samples. For HFO H a more pronounced spread to lower DBE values is observed, indicating a greater proportion of heteroatoms are located in smaller aromatic moieties such as pyridines and pyrroles. For HFOs D and E these fragments typically also have carbon number in excess of 35, suggesting a greater degree of alkylation which may improve their handling properties, such as easier blending with distillates. While it is possible for high DBE nitrogen-containing class fragments to be derived from archipelago-type asphaltene precursors, the alkyl linkage is likely to be cleaved during IRMPD fragmentation, so they can therefore be considered component moieties of island-type asphaltene precursors. Relatively high DBE N[H] class species were also detected in HFO G, while N_2[H] class species concentrated at higher DBE were detected in HFOs B, C, D, and G, spreading to lower DBE values in HFOs E and H. The N_2[H] class fragments of HFO F are at predominantly higher DBE and carbon number, representing content in large aromatic cores,

however the predominant N and N[H] fragments spread to lower DBE values representing content in smaller aromatic moieties, including pyridinic and pyrrolic structures.Generally, the mean DBE was lower in the HC and HC[H] fragment classes for HFOs C, D, E, and H, compared to those for A, B, and G, demonstrating that the degree of condensation in the hydrocarbon fragments generated differs between these groups of samples.

Higher DBE fragments in hydrocarbon classes are indicative of highly condensed aromatic structures, likely to be to incompatible in bulk HFO blends [14, 55]. In general, fragments with DBE in excess of 25 were assigned to odd-electron nitrogen-containing classes in HFOs that present fewer asphaltene handling issues. Conversely, more problematic HFOs generally have the higher DBE fragments predominantly in even-electron nitrogen-containing classes, which may correspond to polar protic and basic compounds, prone to inhibiting hydrotreatment processes [23]. Archipelago-type have lower steric hindrance than island-type asphaltenes and are capable of reorientating individual aromatic cores. Therefore, HFOs that contain a higher proportion of polar heteroatom-containing archipelago-type asphaltenes may have a greater propensity asphaltene handling issues including flocculation, deposition, and inhibition of treatment processes.

3.3 PCA and HCA Analyses

Comparing MS/MS data between multiple samples is time consuming and makes cross referencing challenging. PCA and HCA analyses have been identified as suitable methods for comparing multiple petroleum data sets rapidly [44, 45, 49, 56, 57], and are here applied for the first time to fragment ion data.

For broadband asphaltene and IRMPD fragmentation data, classes were grouped depending on heteroatom content. The results of the PCA and HCA analyses for fragment data are shown in Figures 5 and 6, with the associated variables plot shown in Figure S12. The results of PCA and HCA analyses of the broadband asphaltene spectra are shown in Figures S13-S15. For the fragment data a sufficient proportion of the variance could be explained in the first two principal components (74.2%), while the cophenetic correlation coefficient in HCA analysis was 0.96, confirming efficient clustering [58, 59].

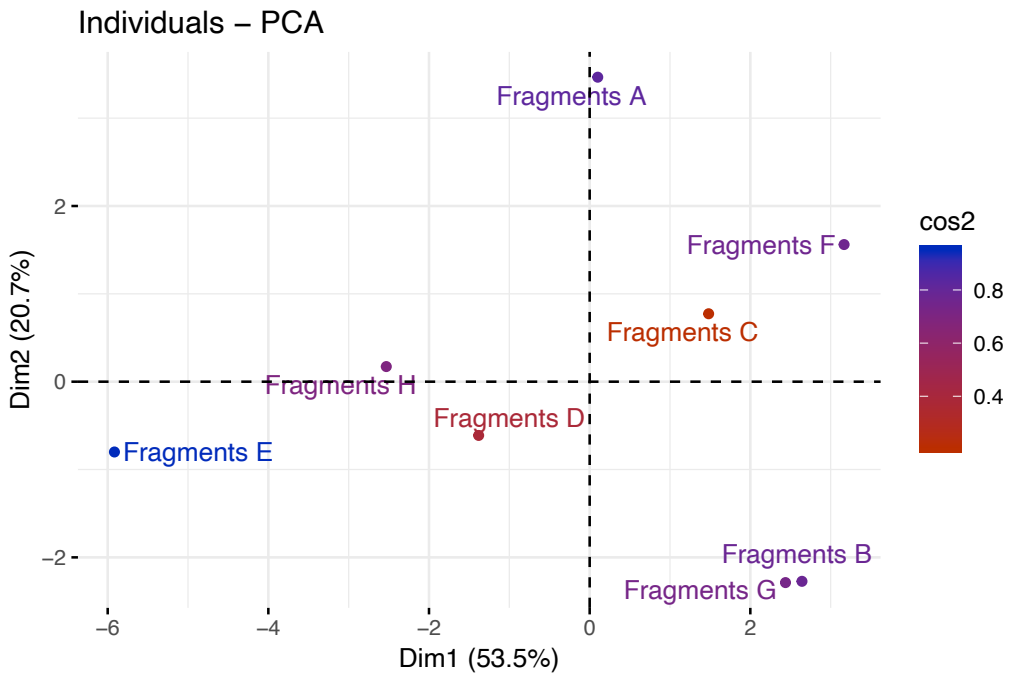

Figure 5 – PCA analysis for grouped compound class IRMPD fragment data.

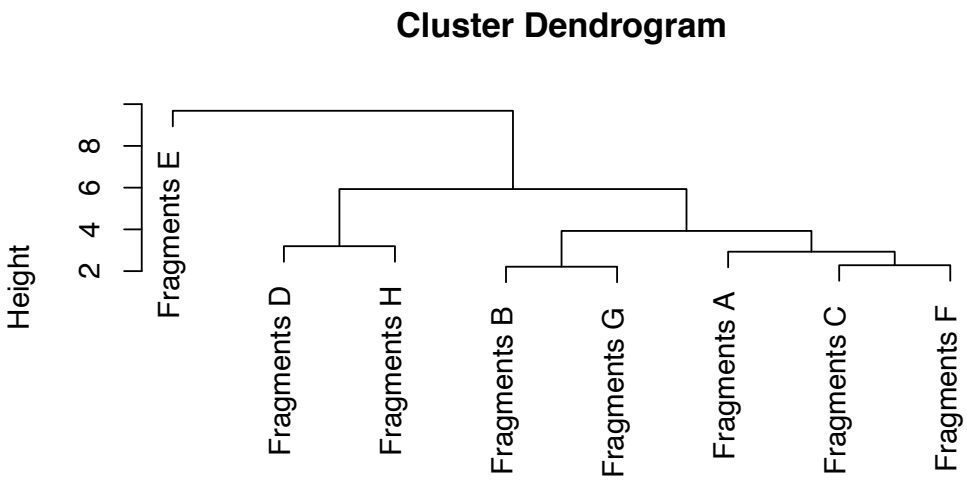

Figure 6 - HCA analysis for grouped compound class IRMPD fragment data

The PCA and HCA analyses are consistent but display some complementary information that provides insight into variations in HFO bulk behaviour. Figure 5 suggests that the asphaltene fragments of HFOs B and G, and to a lesser extent HFOs A, C, and F, and HFOs D, E, and H, group closely. Figure 6 corroborates a greater degree of similarity between HFOs B and G, but suggests that HFO E is less similar to the other samples while HFO A groups less closely to HFOs C and F than they do to one another.

Inspection of the variables loading plot shown in Figure S12 suggests that the grouping of D, E, and H is due to contributions from O_x[H] and NO_x[H] fragments. The NO_x[H] class group variable is located close to the circle of correlations [51] due to its relatively strong contribution to the second principal component, suggesting that the presence of this class at higher relative abundance may be linked to easier handling. HFOs C and F group closely due to contributions from the NO_xS and N_nS_y odd- and even-electron fragments, whereas HFO A appears to differ slightly from these through NO_x class content. The fragments of B and G

appear to be similar based on HC, S_y, and S_y[H] class contributions, reflecting the similarity in the change in compound class group relative intensities observed in Figure 3, yet extending understanding with complementary insight. As the S_y[H] class group contributes most strongly to the first principal component and is located closest to the circle of correlations, it is likely that a high relative abundance of this class may be linked to a higher likelihood of asphaltene handling issues.

The PCA and HCA analysis of fragment spectra can be combined with DBE distributions shown in Figure 4 to improve molecular-level understanding. The statistical analyses provides valuable information, where differences in behaviour cannot be explained by bulk asphaltene content (Table S1) alone. In particular, the PCA indicates that similarities in HC, S, and S[H] class asphaltene fragments may underly problematic behaviour observed in both HFOs B and G despite differences in bulk asphaltene content. While HFO A appears to vary greatly from all other HFO samples in the whole asphaltene PCA shown in Figure S13, due to contributions from the NS[H] and NO_xS[H] classes, species assigned to these classes are also detected in the fragment spectra of HFOs C and F. However, fragment PCA analysis indicates that what sets the fragments of HFO A apart is NO_x content. Cross-referencing with the Figure 4 suggests that these species are found in stable aromatic cores with neutral DBE ranging predominantly between 15 and 27. The broadband asphaltene PCA and HCA groups HFOs B, F, and G closely, although it is known that HFO F presents fewer asphaltene handling problems. The fragment PCA suggests that this may be due to the presence of nitrogen-containing species that form odd-electron fragments in highly condensed stable aromatic cores of HFO F, while a higher proportion of S and high DBE hydrocarbon fragments are observed in HFOs B and G. The asphaltene PCA groups HFOs C, D, E and H closely, largely due to the relative proportions of

several oxygen-containing groups; the fragment PCA provides additional insight. The variation separating HFO C is contributions from nitrogen and sulfur-containing class groups, and that separating HFO E from the other samples is a strong contribution from O_x[H] classes.

4. Conclusion

The combined analytical approach, summarized below, provides a novel and comprehensive means by which to simultaneously compare the asphaltene fractions of marine HFOs.

- Soxhlet extraction was used to isolate the n-heptane insoluble fraction of eight HFOs (C_7 Soxhlet asphaltenes).
- The fractions were dissolved in toluene and studied using (+) APPI-FTICR MS, which provided efficient and preferential compositional access to asphaltenes. Such an approach remains useful for identifying molecular-level differences that may be responsible for varying bulk behaviour and responsiveness to additive packages.
- Fragmentation using IRMPD provided greater insight into asphaltene structure, particularly the predominant situation of heteroatoms in aromatic cores, linking to differences in functionality and bulk properties
- Comparison of DBE and carbon number distributions for multiple compound classes is made possible utilising novel visualization tools, allowing heteroatom situation and the relative degree of aromaticity and alkylation to be compared between the fragments generated for the asphaltenes in several HFOs simultaneously.
- Combining grouped IRMPD fragment data with PCA and HCA analyses identified variables that may underly similarities and differences in HFO bulk behaviour that are

not be immediately obvious. This is pertinent as comparing multiple class distributions and cross-referencing becomes increasingly inefficient and unfeasible for complex data.

The approach presented offers molecular-level compositional insights that are only possible using ultrahigh resolution mass spectrometry. The results further the development and application of the most suitable additives to tackle asphaltene handling issues, and inform future strategies for addressing real world challenges. The methodology may also be applied to the characterisation of crude oil and heavy petroleum, including environmental samples such as oil-sands bitumen, as well as more generally to fragmentation spectra where comparison of molecular-level characteristics is of interest.

Acknowledgements

Mary J. Thomas, Hugh E. Jones, and Rémy Gavard thank EPSRC for a PhD studentship through the EPSRC Centre for Doctoral Training in Molecular Analytical Science (grant number EP/L015307/1).

Diana Catalina Palacio Lozano thanks the Newton Fund award (reference number 275910721), Research Agreement No. 5211770 UIS-ICP, and COLCIENCIAS (project No. FP44842-039-2015).

The authors would also like to thank David Stranz, Sierra Analytics, for developments and access to Composer software.

The authors publish with permission of Lubrizol Ltd.

References

[1] Palacio Lozano DC, Gavard R, Arenas-Diaz JP, Thomas MJ, Stranz DD, Mejía-Ospino E, et al. Pushing the analytical limits: new insights into complex mixtures using mass spectra segments of constant ultrahigh resolving power. Chemical Science 2019;10(29):6966-78.

[2] Schmidt EM, Pudenzi MA, Santos JM, Angolini CFF, Pereira RCL, Rocha YS, et al. Petroleomics via Orbitrap mass spectrometry with resolving power above 1 000 000 at m/z 200. Rsc Advances 2018;8(11):6183-91.

[3] Rüger CP, Sklorz M, Schwemer T, Zimmermann R. Characterisation of ship diesel primary particulate matter at the molecular level by means of ultra-high-resolution mass spectrometry coupled to laser desorption ionisation—comparison of feed fuel, filter extracts and direct particle measurements. Analytical and Bioanalytical Chemistry 2015;407(20):5923-37.

[4] Akbarzadeh K, Hammami A, Kharrat A, Zhang D, Allenson S, Creek J, et al. Asphaltenes - Problematic but Rich in Potential. Oilfield Review 2007;19(2):22-43.

[5] Sheu EY, Storm DA. Colloidal Properties of Asphaltenes in Organic Solvents. In: Sheu EY, Mullins OC, editors. Asphaltenes: Fundamentals and Applications. Boston, MA: Springer US; 1995, p. 1-52.

[6] Wiehe IA. Process Chemistry of Petroleum Macromolecules. FL: CRC Press: Boca Raton; 2008.

[7] Durand E, Clemancey M, Lancelin JM, Verstraete J, Espinat D, Quoineaud AA. Effect of Chemical Composition on Asphaltenes Aggregation. Energy & Fuels 2010;24(2):1051-62.

[8] Wiehe IA, Kennedy RJ. The oil compatibility model and crude oil incompatibility. Energy & Fuels 2000;14(1):56-9.

[9] Vermeire MB. Everything You Need to Know About Marine Fuels. Chevron Global Marine Products; 2012.

[10] Jameel AGA, Khateeb A, Elbaz AM, Emwas AH, Zhang W, Roberts WL, et al. Characterization of deasphalted heavy fuel oil using APPI (+) FT-ICR mass spectrometry and NMR spectroscopy. Fuel 2019;253:950-63.

[11] Kabel K, Abdelghaffar A, Farag R, Maysour N, Zahran M. Synthesis and evaluation of PAMAM dendrimer and PDPF-b-POP block copolymer as asphaltene inhibitor/dispersant. Research on Chemical Intermediates 2015;41(1):457-74.

[12] Le Lannic K, Guibard I, Merdrignac I. Behavior and role of asphaltenes in a two-stage fixed bed hydrotreating process. Petroleum Science and Technology 2007;25(1-2):169-86.

[13] Halff A, Younes L, Boersma T. The likely implications of the new IMO standards on the shipping industry. Energy Policy 2019;126:277-86.

[14] Zeuthen P, Knudsen KG, Whitehurst DD. Organic nitrogen compounds in gas oil blends, their hydrotreated products and the importance to hydrotreatment. Catalysis Today 2001;65(2-4):307-14.
[15] Guillemant J, Albrieux F, Lacoue-Negre M, de Oliveira LP, Joly JF, Duponchel L. Chemometric Exploration of APPI(+)-FT-ICR MS Data Sets for a Comprehensive Study of Aromatic Sulfur Compounds in Gas Oils. Analytical Chemistry 2019;91(18):11785-93.
[16] Kafer U, Groger T, Ruger CP, Czech H, Saraji-Bozorgzad M, Wilharm T, et al. Direct inlet probe - High-resolution time-of-flight mass spectrometry as fast technique for the chemical description of complex high-boiling samples. Talanta 2019;202:308-16.
[17] Bukowski A, Milczarska T. ASPHALTS AS INHIBITORS OF RADICAL POLYMERIZATION. Journal of Applied Polymer Science 1983;28(3):1001-9.
[18] McGill WB, Rowell MJ. DETERMINATION OF OIL CONTENT OF OIL CONTAMINATED SOIL. Science of the Total Environment 1980;14(3):245-53.
[19] Thomas MJ, Collinge E, Witt M, Lozano DCP, Vane CH, Moss-Hayes V, et al. Petroleomic depth profiling of Staten Island salt marsh soil: 2 omega detection FTICR MS offers a new solution for the analysis of environmental contaminants. Science of the Total Environment 2019;662:852-62.
[20] Dickie JP, Yen TF. Macrostructures of the asphaltic fractions by various instrumental methods. Analytical Chemistry 1967;39(14):1847-52.
[21] Mullins OC, Sabbah H, Eyssautier J, Pomerantz AE, Barre L, Andrews AB, et al. Advances in Asphaltene Science and the Yen-Mullins Model. Energy & Fuels 2012;26(7):3986-4003.
[22] Mullins OC. The Asphaltenes. In: Cooks RG, Yeung ES, editors. Annual Review of Analytical Chemistry, Vol 4. 2011, p. 393-418.
[23] Guillemant J, Albrieux F, de Oliveira LP, Lacoue-Negre M, Duponchel L, Joly JF. Insights from Nitrogen Compounds in Gas Oils Highlighted by High-Resolution Fourier Transform Mass Spectrometry. Analytical Chemistry 2019;91(20):12644-52.
[24] Nyadong L, Lai JF, Thompsen C, LaFrancois CJ, Cai XH, Song CX, et al. High-Field Orbitrap Mass Spectrometry and Tandem Mass Spectrometry for Molecular Characterization of Asphaltenes. Energy & Fuels 2018;32(1):294-305.
[25] Tang WJ, Hurt MR, Sheng HM, Riedeman JS, Borton DJ, Slater P, et al. Structural Comparison of Asphaltenes of Different Origins Using Multi-stage Tandem Mass Spectrometry. Energy & Fuels 2015;29(3):1309-14.
[26] Chacon-Patino M, Rowland S, Rodgers R. Advances in Asphaltene Petroleomics. Part 1: Asphaltenes Are Composed of Abundant Island and Archipelago Structural Motifs. Energy & Fuels 2017;31(12):13509-18.
[27] Chacon-Patino ML, Rowland SM, Rodgers RP. Advances in Asphaltene Petroleomics. Part 2: Selective Separation Method That Reveals Fractions Enriched in Island and Archipelago Structural Motifs by Mass Spectrometry. Energy & Fuels 2018;32(1):314-28.
[28] Chacon-Patino ML, Rowland SM, Rodgers RP. Advances in Asphaltene Petroleomics. Part 3. Dominance of Island or Archipelago Structural Motif Is Sample Dependent. Energy & Fuels 2018;32(9):9106-20.
[29] Ruger CP, Neumann A, Sklorz M, Schwemer T, Zimmermann R. Thermal Analysis Coupled to Ultrahigh Resolution Mass Spectrometry with Collision Induced

Dissociation for Complex Petroleum Samples: Heavy Oil Composition and Asphaltene Precipitation Effects. Energy & Fuels 2017;31(12):13144-58.
[30] Santos JM, Wisniewski A, Eberlin MN, Schrader W. Comparing Crude Oils with Different API Gravities on a Molecular Level Using Mass Spectrometric Analysis. Part 1: Whole Crude Oil. Energies 2018;11(10).
[31] Farenc M, Corilo YE, Lalli PM, Riches E, Rodgers RP, Afonso C, et al. Comparison of Atmospheric Pressure Ionization for the Analysis of Heavy Petroleum Fractions with Ion Mobility-Mass Spectrometry. Energy & Fuels 2016;30(11):8896-903.
[32] Zhang YH, Zhang LZ, Xu ZM, Zhang N, Chung KH, Zhao SQ, et al. Molecular Characterization of Vacuum Resid and Its Fractions by Fourier Transform Ion Cyclotron Resonance Mass Spectrometry with Various Ionization Techniques. Energy & Fuels 2014;28(12):7448-56.
[33] Pereira TMC, Vanini G, Oliveira ECS, Cardoso FMR, Fleming FP, Neto AC, et al. An evaluation of the aromaticity of asphaltenes using atmospheric pressure photoionization Fourier transform ion cyclotron resonance mass spectrometry - APPI(+/-)FT-ICR MS. Fuel 2014;118:348-57.
[34] Santos JM, Vetere A, Wisniewski A, Eberlin MN, Schrader W. Comparing Crude Oils with Different API Gravities on a Molecular Level Using Mass Spectrometric Analysis. Part 2: Resins and Asphaltenes. Energies 2018;11(10).
[35] Cho Y, Birdwell JE, Hur M, Lee J, Kim B, Kim S. Extension of the Analytical Window for Characterizing Aromatic Compounds in Oils Using a Comprehensive Suite of High-Resolution Mass Spectrometry Techniques and Double Bond Equivalence versus Carbon Number Plot. Energy & Fuels 2017;31(8):7874-83.
[36] Annesley TM. Ion suppression in mass spectrometry. Clinical Chemistry 2003;49(7):1041-4.
[37] Hanold KA, Fischer SM, Cormia PH, Miller CE, Syage JA. Atmospheric pressure photoionization. 1. General properties for LC/MS. Analytical Chemistry 2004;76(10):2842-51.
[38] McLafferty FW. A Century of Progress in Molecular Mass Spectrometry. Annual Review of Analytical Chemistry 2011;4(1):1-22.
[39] Mayer PM, Poon C. THE MECHANISMS OF COLLISIONAL ACTIVATION OF IONS IN MASS SPECTROMETRY. Mass Spectrometry Reviews 2009;28(4):608-39.
[40] Douglas DJ. Applications of Collision Dynamics in Quadrupole Mass Spectrometry. Journal of the American Society for Mass Spectrometry 1998;9(2):101-13.
[41] Payne AH, Glish GL. Thermally assisted infrared multiphoton photodissociation in a quadrupole ion trap. Analytical Chemistry 2001;73(15):3542-8.
[42] Little DP, Speir JP, Senko MW, Oconnor PB, McLafferty FW. INFRARED MULTIPHOTON DISSOCIATION OF LARGE MULTIPLY-CHARGED IONS FOR BIOMOLECULE SEQUENCING. Analytical Chemistry 1994;66(18):2809-15.
[43] Polfer NC. Infrared multiple photon dissociation spectroscopy of trapped ions. Chemical Society Reviews 2011;40(5):2211-21.
[44] Stout SA, Uhler AD, McCarthy KJ. A Strategy and Methodology for Defensibly Correlating Spilled Oil to Source Candidates. Environmental Forensics 2001;2(1):87-98.
[45] Hur M, Yeo I, Park E, Kim Y, Yoo J, Kim E, et al. Combination of Statistical Methods and Fourier Transform Ion Cyclotron Resonance Mass Spectrometry for More

Comprehensive, Molecular-Level Interpretations of Petroleum Samples. Analytical Chemistry 2010;82(1):211-8.
[46] Krajewski LC, Lobodin VV, Johansen C, Bartges TE, Maksimova EV, MacDonald IR, et al. Linking Natural Oil Seeps from the Gulf of Mexico to Their Origin by Use of Fourier Transform Ion Cyclotron Resonance Mass Spectrometry. Environmental Science & Technology 2018;52(3):1365-74.
[47] Chiaberge S, Fiorani T, Savoini A, Bionda A, Ramello S, Pastori M, et al. Classification of crude oil samples through statistical analysis of APPI FTICR mass spectra. Fuel Processing Technology 2013;106:181-5.
[48] Islam A, Ahmed A, Hur M, Thorn K, Kim S. Molecular-level evidence provided by ultrahigh resolution mass spectrometry for oil-derived doc in groundwater at Bemidji, Minnesota. Journal of Hazardous Materials 2016;320:123-32.
[49] Lozano DCP, Orrego-Ruiz JA, Hernandez RC, Guerrero JE, Mejia-Ospino E. APPI(+)-FTICR mass spectrometry coupled to partial least squares with genetic algorithm variable selection for prediction of API gravity and CCR of crude oil and vacuum residues. Fuel 2017;193:39-44.
[50] Barrow M, Headley J, Peru K, Derrick P. Data Visualization for the Characterization of Naphthenic Acids within Petroleum Samples. Energy & Fuels 2009;23(5-6):2592-9.
[51] Abdi H, Williams LJ. Principal component analysis. Wiley Interdisciplinary Reviews: Computational Statistics 2010;2(4):433-59.
[52] Boukherissa M, Mutelet F, Modarressi A, Dicko A, Dafri D, Rogalski M. Ionic Liquids as Dispersants of Petroleum Asphaltenes. Energy & Fuels 2009;23(5):2557-64.
[53] Amer MW, Marshall M, Fei Y, Jackson WR, Gorbaty ML, Cassidy PJ, Chaffee AL. The structure and reactivity of a low-sulfur lacustrine oil shale (Colorado U.S.A.) compared with those of a high-sulfur marine oil shale (Julia Creek, Queensland, Australia). Fuel Processing Technology 2015, 135, 91-90
[54] Cho YJ, Na JG, Nho NS, Kim S. Application of Saturates, Aromatics, Resins, and Asphaltenes Crude Oil Fractionation for Detailed Chemical Characterization of Heavy Crude Oils by Fourier Transform Ion Cyclotron Resonance Mass Spectrometry Equipped with Atmospheric Pressure Photoionization. Energy & Fuels 2012;26(5):2558-65.
[55] Gabrienko AA, Subramani V, Martyanov ON, Kazarian SG. Correlation between Asphaltene Stability in n-Heptane and Crude Oil Composition Revealed with In Situ Chemical Imaging. Adsorption Science & Technology 2014;32(4):243-55.
[56] Grewer DM, Young RF, Whittal RM, Fedorak PM. Naphthenic acids and other acid-extractables in water samples from Alberta: What is being measured? Science of the Total Environment 2010;408(23):5997-6010.
[57] Headley J, Barrow M, Peru K, Fahlman B, Frank R, Bickerton G, et al. Preliminary fingerprinting of Athabasca oil sands polar organics in environmental samples using electrospray ionization Fourier transform ion cyclotron resonance mass spectrometry. Rapid Communications in Mass Spectrometry 2011;25(13):1899-909.
[58] Sokal R, Rohlf F. Sokal RR, Rohlf FJ. The comparison of dendrograms by objective methods. Taxon 11: 33-40. Taxon 1962;11:33-40.
[59] Saraçli S, Doğan N, Doğan İ. Comparison of hierarchical cluster analysis methods by cophenetic correlation. Journal of Inequalities and Applications 2013;2013(1):203.